ChemComm

COMMUNICATION

View Article Online
View Journal | View Issue

Cite this: *Chem. Commun.*, 2019, **55**, 15045

Received 14th November 2019,
Accepted 22nd November 2019

DOI: 10.1039/c9cc08895d

rsc.li/chemcomm

A general strategy to develop cell membrane fluorescent probes with location- and target-specific fluorogenicities: a case of a Zn^{2+} probe with cellular selectivity†

Fei Deng,[ab] Limin Liu,[a] Qinglong Qiao,*[b] Chunfang Huang,[a] Lu Miao[b] and Zhaochao Xu *[b]

We reported fluorescent probes to image Zn^{2+} with plasma membrane-specific and Zn^{2+}-specific fluorogenicities. The probes contained hydrophobic alkyl chains as membrane-anchored domains and hydrophilic zinc sensor ZTRS, and aggregated to display quenched fluorescence. Cells dissolved the aggregates and the liberated probes were dispersed on the outside of the cell plasma membrane. Aggregates that did not bind to the cell membrane still exhibited aggregation-induced fluorescence quenching after complexing with zinc ions, while probes anchored on the membrane surface exhibited a fluorescence-enhanced response upon recognition of zinc ions.

The emergence of new fluorescence imaging techniques has facilitated the development of fluorescent probes to monitor the subcellular localization and dynamics of biological targets.[1–3] These probes derived from organic fluorescent dyes are attractive alternatives to fluorescent proteins, profiting from their small size, good photophysical properties and emissions spanning the color spectra.[4] But an inherent disadvantage of organic fluorophores is that they are not genetically encoded and cannot be accurately located and quantified. These unbound or location-unspecific probes can produce background interference. To address this issue, fluorogenic probes have been developed, which are initially fluorescence-silent, but activated upon target recognition with specific fluorescence responses.[5,6]

Fluorogenic probes are powerful tools to image analytes having a fixed location, such as biological macromolecules like enzymes[5] or cellular structural units like the cytoskeleton.[6] The probe needs to have a locational targeting ability and a selective fluorescence recognition ability to the analyst (namely target-specific fluorogenicity). Even if the excessive probes are distributed in the wrong location, the interference fluorescence signal will not be produced because the analyte will not appear around the location-unspecific probes. However, for analytes that exist everywhere in the spatial distribution, such as free metal ions or biological parameters such as polarity or viscosity, probes must have a so-called location-specific fluorogenicity in addition to target-specific fluorogenicity to ensure those location-unspecific probes do not have fluorescence recognition after binding the analyte.[7,8]

Cell membrane probes can be used as a typical example to explain the need for both location- and target-specific fluorogenicities.[9–13] If it is only used to track the dynamic changes of the cell membrane itself,[9–11] the probe only needs to have a fluorescent recognition such as fluorescence enhancement after binding to the cell membrane. However, if it is used to monitor the transport of substances inside or outside the cell membrane, the probe needs to be quantitatively anchored to the cell membrane or it is required that only the probe anchored to the cell membrane has fluorescence recognition ability (namely location-specific fluorogenicity). In order to obtain a location-specific fluorogenicity, current cell membrane probes mainly depend on the removal of probes that are not anchored to the cell membrane by screening the amount of probes and washing them after co-culture with the cells. Therefore, real-time *in situ* dynamic imaging of extracellular molecule release in intact cells requires a new probe design strategy to achieve both location- and target-specific fluorogenicities.

In this paper, we used the aggregation–disaggregation strategy to achieve the membrane-specific fluorogenicity of the probe (Fig. 1). Zinc is an essential trace element distributed unevenly in living organisms. The transient increases of free Zn^{2+} are regarded as signals in inter- and intracellular communication. More specifically, these trans-membrane signals include Zn^{2+} efflux during nerve impulses in neurons,[14] Zn^{2+} release coupled with insulin secretion in pancreatic islet β cells,[15] and Zn^{2+} sparks in the mammalian egg to embryo transition.[16] Fluorescent probes for monitoring zinc release from living cells have been constructed by combining zinc sensing domains with membrane-anchored groups through hydrophobic interactions[17–21] or genetically encoded bioorthogonal reactions.[22] In our previous work, we reported an amide-containing DPA chelator

[a] *School of Chemistry and Chemical Engineering, Jinggangshan University, Ji'an, Jiangxi 343009, China*
[b] *CAS Key Laboratory of Separation Science for Analytical Chemistry, Dalian Institute of Chemical Physics, Chinese Academy of Sciences, Dalian 116023, China. E-mail: qqlqiao@dicp.ac.cn, zcxu@dicp.ac.cn*

† Electronic supplementary information (ESI) available. See DOI: 10.1039/c9cc08895d

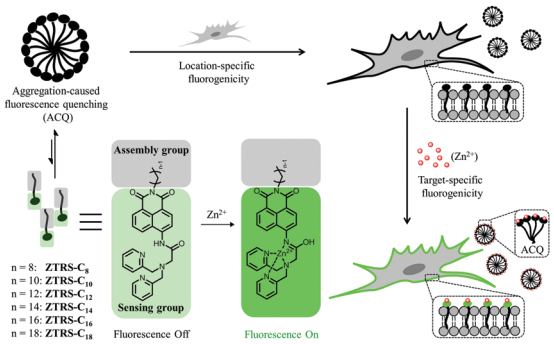

Fig. 1 The design of a fluorogenic probe for imaging Zn^{2+} at the surface of the plasma membrane of living cells.

ZTRS as a highly selective probe for Zn^{2+}.[23] In this paper, we introduced hydrophobic alkyl chains as membrane-anchored domains into **ZTRS**. The new feature of the probes, as shown in Fig. 1, was that they aggregated and exhibited aggregation-caused fluorescence quenching (ACQ). The formed nano-particles would be disaggregated by the interaction with cells and the liberated probes were dispersed on the outside of the cell plasma membrane. Aggregates that do not bind to the cell membrane still exhibit aggregation-induced quenched fluorescence after complexing with zinc ions, while probes anchored on the membrane surface exhibit a fluorescence-enhanced response upon recognition of zinc ions. Thus, the aggregation–disaggregation strategy gives plasma membrane probes abilities of location- and target-specific fluorogenicities.

This strategy needs to meet three requirements: the first is that the probe aggregates in aqueous solution and exhibits aggregation-caused fluorescence quenching; the second is that the cell is capable of dissolving the aggregates; the third is that the analyte has no ability to dissociate the aggregates. The octadecyl-derived **ZTRS** has been proven to aggregate and exhibit quenched fluorescence after binding zinc ions.[24] In order to further screen out a molecule that satisfied the above three requirements, we introduced alkyl chains of different lengths into **ZTRS**. A series of Zn^{2+} probes named **ZTRS-alkyl** were synthesized (Fig. 1 and ESI†).

The fluorescence responses of these probes to Zn^{2+} in aqueous solutions were first examined. As shown in Fig. 2a, the octyl- and decyl-substituted **ZTRS-C$_8$** and **ZTRS-C$_{10}$** displayed obvious fluorescence increase with the addition of zinc ions, while dodecyl-, tetradecyl, hexadecyl- and octadecyl-substituted **ZTRS-C$_{12}$**, **ZTRS-C$_{14}$**, **ZTRS-C$_{16}$** and **ZTRS-C$_{18}$** displayed nominal changes of fluorescence intensities. Significantly, the addition of zinc ions red-shifted the emission of all these six compounds (Fig. S1–S6, ESI†). The red-shifted emission indicated that these compounds bound zinc ions in an imidic acid tautomeric form of the amide-DPA receptor. The nano-structures of **ZTRS-C$_8$** (Fig. S7, ESI†) and **ZTRS-C$_{18}$** indicated that all probes could form similar aggregates in aqueous solution.[24] However, the complexing of zinc ions dissolved the aggregates of **ZTRS-C$_8$** and **ZTRS-C$_{10}$** without unravelling aggregates of **ZTRS-C$_{12}$**, **ZTRS-C$_{14}$**, **ZTRS-C$_{16}$** and **ZTRS-C$_{18}$**. To demonstrate that the disassembly of the nano-aggregates was the key point of the

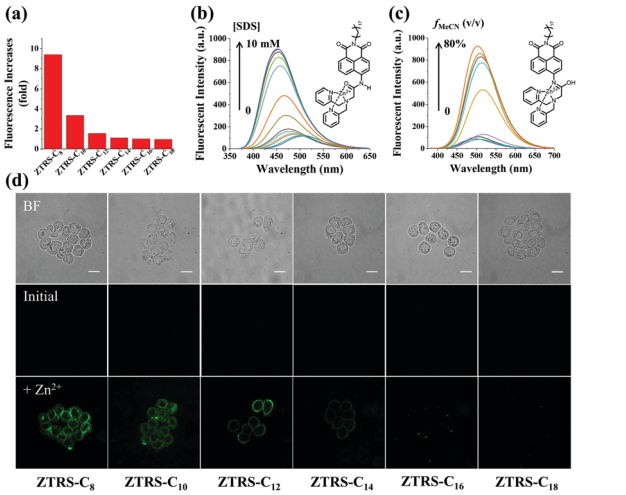

Fig. 2 (a) Fluorescence responses of 10 μM **ZTRS-alkyl** compounds (20 mM HEPES, pH 7.4) with the addition of 30 μM Zn^{2+}. (b) Fluorescence spectra of 10 μM **ZTRS-C$_{18}$** and 30 μM Zn^{2+} with the addition of different concentrations of SDS (20 mM HEPES, pH 7.4). (c) Fluorescence spectra of 10 μM **ZTRS-C$_{18}$** and 30 μM Zn^{2+} in mixed solvents of 20 mM HEPES (pH 7.4) with different volume fractions of CH_3CN. (d) Confocal fluorescence image of HT-29 cells loaded with 5 μM **ZTRS-alkyl** compounds. Upper: bright field; middle: fluorescence imaging of cells stained with 5 μM **ZTRS-alkyl** compounds for 30 min; bottom: fluorescence imaging of cells after addition of 50 μM Zn^{2+} for 10 min. Ex: 405 nm; slit: 500–550 nm; scale bar: 20 μm.

location-specific fluorogenicity, we added surfactants or CH_3CN to the aqueous solutions of **ZTRS-C$_{18}$** (Fig. 2b and c). The obvious fluorescence increase revealed that both surfactants and cosolvents could disperse the nano-aggregates and induce fluorescence enhancement. It is worth noting that **ZTRS-C$_{18}$-Zn(II)** is environment sensitive. The emission maxima of solutions with SDS or CH_3CN were 450 and 525 nm, which corresponded to amide and imidic acid tautomeric forms, respectively.

The results mentioned above inspired us to conduct further cell staining experiments to study the location- and target-specific fluorogenicities of these compounds to the plasma membrane. As shown in Fig. 2d, in the presence of Zn^{2+}, HT-29 cells stained with **ZTRS-C$_8$**, **ZTRS-C$_{10}$** and **ZTRS-C$_{12}$** exhibited strong emission. But only for the cells stained with **ZTRS-C$_{12}$** can it be seen that the fluorescence was emitted from the cell membrane region as determined by confocal scanning laser microscopy, and the cells stained with **ZTRS-C$_8$** and **ZTRS-C$_{10}$** also emitted fluorescence inside. Cells stained with **ZTRS-C$_{14}$** exhibited weak emission, while those stained with **ZTRS-C$_{16}$** and **ZTRS-C$_{18}$** did not give any fluorescence signals. We concluded that the quenched fluorescence in **ZTRS-C$_{16}$** and **ZTRS-C$_{18}$** might be attributed to the strong hydrophobicity of the hexadecyl and octadecyl alkyl chain. Cells could hardly disperse the nano-aggregates like micelles formed by surfactants. Reducing the hydrophobicity of alkyl chains might facilitate the dispersion of probes to dissolve in the plasma membrane. Since the experiments in aqueous solution and cell staining showed that **ZTRS-C$_{12}$** had superiority in plasma membrane location and fluorogenicity over other probes mentioned above, we conducted further study based on the compound **ZTRS-C$_{12}$**.

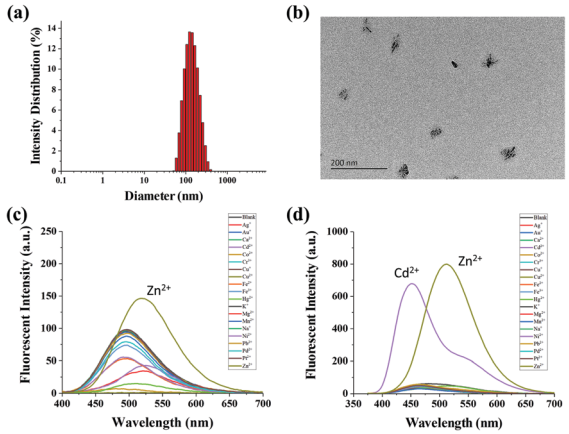

Fig. 3 (a) DLS analysis of particle-size distribution of the self-assembled **ZTRS-C$_{12}$** (10 μM) in 20 mM HEPES (pH 7.4). (b) TEM image of the self-assembled **ZTRS-C$_{12}$**. (c) Fluorescence spectra of 10 μM **ZTRS-C$_{12}$** in the presence of 30 μM various metal ions in 20 mM HEPES (pH 7.4). (d) Fluorescence spectra of 10 μM **ZTRS-C$_{12}$** in the presence of 30 μM various metal ions in a mixed solvent system consisting of 50% 20 mM HEPES (pH = 7.4) and 50% acetonitrile (v/v).

The aggregation of **ZTRS-C$_{12}$** in aqueous solution was demonstrated and evaluated with the means of dynamic light scattering (DLS) measurements and transmission electron microscopy (TEM) (Fig. 3a and b). DLS analysis showed the aggregates with a diameter of mean size 120 nm (Fig. 3a), which was larger than 50 nm measured in TEM experiments (Fig. 3b). This was mainly attributed to the different state measured in DLS and TEM. TEM depicted the actual size at the dried state of the sample, whereas DLS measured the hydrodynamic size.[25]

In our previous report, **ZTRS** showed excellent selectivity for Zn^{2+} over most competitive heavy and transition metal ions.[23] We also checked the selectivity of **ZTRS-C$_{12}$** for Zn^{2+}. In HEPES buffer solutions, the addition of Zn^{2+} only induced a fluorescent intensity increase of 1.5 folds and the maximum emission red-shifted from 496 nm to 519 nm (Fig. 3c). The addition of other metal ions quenched the fluorescence to different extents. We also added metal ions to mixed solutions of HEPES buffer with CH_3CN (v/v = 1 : 1) to examine the selectivity of **ZTRS-C$_{12}$**. We got fluorescence responses similar to that of **ZTRS** (Fig. 3d). With the addition of Zn^{2+} to the solution of **ZTRS-C$_{12}$**, a characteristic red-shift in emission and an obvious intensity increase (13 fold) were observed. Cd^{2+} induced a blue-shift in the emission from 480 nm to 452 nm while Zn^{2+} caused a red-shift to 512 nm. These results verified that the aggregation of **ZTRS-C$_{12}$** controlled the fluorescence recognition properties.

To assess the ability of **ZTRS-C$_{12}$** to respond to the homeostasis of Zn^{2+} at the plasma membrane, we conducted the following competition studies. As shown in Fig. 4, **ZTRS-C$_{12}$** stained HT-29 cells and emitted negligible fluorescence at the plasma membrane. Subsequently, no-wash live-cell fluorescence sensing of zinc at the plasma membrane was carried out. The fluorescence imaging was taken without washing the cells after the addition of Zn^{2+}. Obvious fluorescence was only observed at the cell membrane with slit at

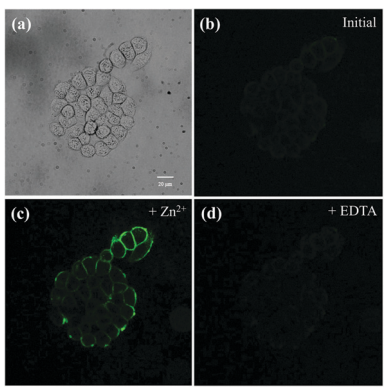

Fig. 4 Fluorescence imaging of Zn^{2+} at the plasma membrane of HT-29 cells. (a) Bright field; (b) initial fluorescence signal of cells stained with 5 μM **ZTRS-C$_{12}$** for 30 min; (c) fluorescence imaging with the addition of 50 μM Zn^{2+} for 10 min; (d) fluorescence imaging with the subsequent addition of 100 μM EDTA for 10 min. Ex: 405 nm; slit: 500–550 nm; scale bar: 20 μm.

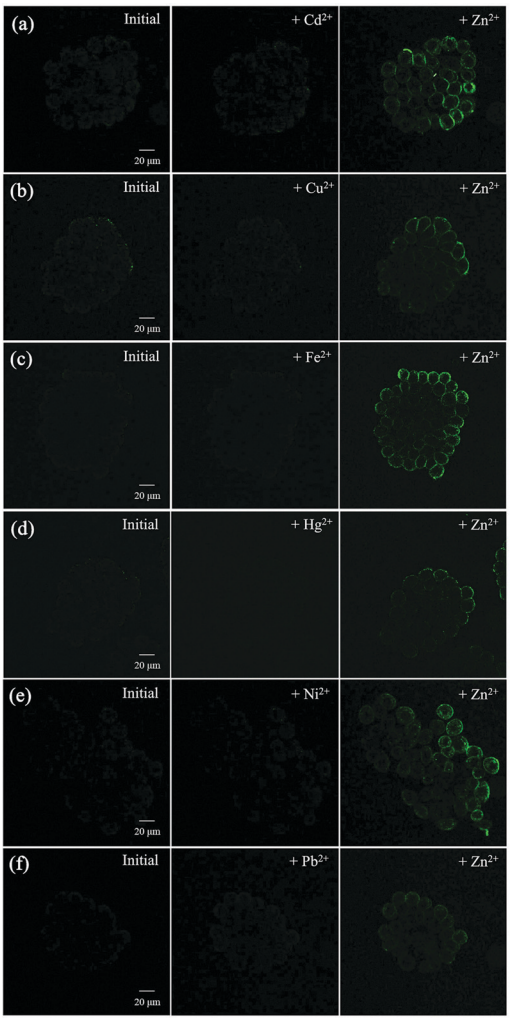

Fig. 5 Fluorescence imaging of extracellular metal ion response in HT-29 cells: (a) Cd^{2+}, (b) Cu^{2+}, (c) Fe^{2+}, (d) Hg^{2+}, (e) Ni^{2+}, (f) Pb^{2+} (a, b, c, d, e, f from left to right: initial fluorescence signal of cells stained with 5 μM **ZTRS-C$_{12}$** for 30 min; fluorescence imaging after the addition of 50 μM Cd^{2+}, Cu^{2+}, Fe^{2+}, Hg^{2+}, Ni^{2+} or Pb^{2+} for 10 min; fluorescence imaging after the addition of 100 μM Zn^{2+} for 10 min). Ex: 405 nm; slit: 500–550 nm; scale bar: 20 μm.

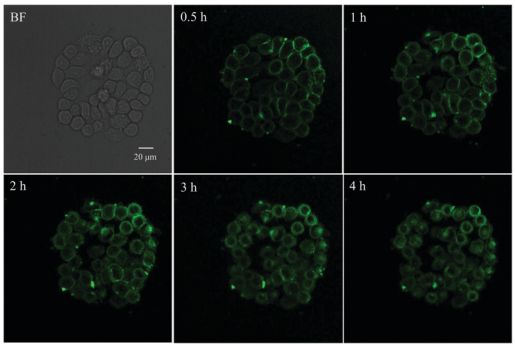

Fig. 6 Location of **ZTRS-C_{12}** in live HT-29 cells after a period of time incubated in a live cell imaging system. 50 μM Zn^{2+} was added before imaging; Ex: 405 nm; slit: 500–550 nm; scale bar: 20 μm.

500–550 nm rather than 417–477 nm (Fig. 3c and Fig. S8, ESI†). With the addition of 100 μM EDTA to displace zinc from the probe complex, the fluorescence signals disappeared. The probe exhibited good cell membrane fluorogenicity and the potential to track the dynamic changes of zinc ions.

We further examined the responses of **ZTRS-C_{12}** to other biologically important heavy and transition metal ions in cells to evaluate its cellular selectivity. As shown in Fig. 5, the addition of Cd^{2+}, Fe^{2+}, Ni^{2+}, Pb^{2+}, Cu^{2+} and Hg^{2+} did not induce any fluorescence enhancement. But the subsequent addition of Zn^{2+} turned on the fluorescence at the plasma membrane region, indicating the displacement of these ions by Zn^{2+}. The high cellular selectivity for zinc ensures the accuracy of the signal obtained when **ZTRS** detects zinc ions in the cells. To the best of our knowledge, most probes evaluate the selectivity of the probe to the analyte in a buffer solution, and have not seen any probes to study selectivity in the cellular environment. Besides, we found that the addition of metal ions, except Fe^{2+}, caused some probes to enter the cell through the cell membrane, which was attributed to the toxicity of these metal ions to change the permeability of the plasma membrane.

With the localization and zinc fluorogenicity of **ZTRS-C_{12}** established, we evaluated the robustness by which our construct labeled the plasma membrane. The plasma membrane consisted of lipid bilayer, which dynamically exchange lipid component with internal membrane through vesicular transport. Probes localized in the plasma membrane would internalize inevitably. The longer time the probe stayed in the plasma membrane, the more practical in imaging. Then we incubated the probe with HT-29 cells and observed through live cell imaging system for a long period. **ZTRS-C_{12}** was retained in the plasma membrane for more than 2 hours and then internalized gradually (Fig. 6), which was comparable to previous reported probes like **Palm-ZP1**.[19]

In conclusion, using a Zn^{2+} probe as an example, we reported an aggregation–disaggregation strategy to develop cell membrane anchored fluorescent probes with both location- and target-specific fluorogenicities. Probes dispersed on the outside of the cell plasma membrane have the ability to selectively sense Zn^{2+} and ensure wash-free fluorescence imaging. This strategy is expected to become a new method for constructing cell membrane probes.

This work was supported by the financial support from the National Natural Science Foundation of China (21878286, 21908216, 21765011).

Conflicts of interest

There are no conflicts to declare.

Notes and references

1 H. Zhu, J. L. Fan, J. J. Du and X. J. Peng, *Acc. Chem. Res.*, 2016, **49**, 2115.
2 P. Gao, W. Pan, N. Li and B. Tang, *Chem. Sci.*, 2019, **10**, 6035.
3 W. Xu, Z. B. Zeng, J. H. Jiang, Y. T. Chang and L. Yuan, *Angew. Chem., Int. Ed.*, 2016, **55**, 13658.
4 L. Wang, M. S. Frei, A. Salim and K. Johnsson, *J. Am. Chem. Soc.*, 2019, **141**, 2770.
5 W. Chyan and R. T. Raines, *ACS Chem. Biol.*, 2018, **13**, 1810.
6 G. Lukinavicius, L. Reymond, E. D'Este, A. Masharina, F. Gutfert, H. Ta, A. Guether, M. Fournier, S. Rizzo, H. Waldmann, C. Blaukopf, C. Sommer, D. W. Gerlich, H. D. Arndt, S. W. Hell and K. Johnsson, *Nat. Methods*, 2014, **11**, 731.
7 S. S. Long, Q. L. Qiao, L. Miao and Z. C. Xu, *Chin. Chem. Lett.*, 2019, **30**, 573.
8 F. Deng and Z. Xu, *Chin. Chem. Lett.*, 2019, **30**, 1667.
9 J. Mu, F. Liu, M. S. Rajab, M. Shi, S. Li, C. Goh, L. Lu, Q. H. Xu, B. Liu, L. G. Ng and B. G. Xing, *Angew. Chem., Int. Ed.*, 2014, **53**, 14357.
10 H. R. Jia, Y. X. Zhu, K. F. Xu, G. Y. Pan, X. Y. Liu, Y. Qiao and F. G. Wu, *Chem. Sci.*, 2019, **10**, 4062.
11 M. H. Lee, H. M. Jeon, J. H. Han, N. Park, C. Kang, J. L. Sessler and J. S. Kim, *J. Am. Chem. Soc.*, 2014, **136**, 8430.
12 M. Niwa, T. Hirayama, I. Oomoto, D. O. Wang and H. Nagasawa, *ACS Chem. Biol.*, 2018, **13**, 1853.
13 S. Xu, H.-W. Liu, X. Yin, L. Yuan, S.-Y. Huan and X.-B. Zhang, *Chem. Sci.*, 2019, **10**, 320.
14 Y. Qin, D. Thomas, C. P. Fontaine and R. A. Colvin, *Neurosci. Lett.*, 2009, **450**, 206.
15 G. A. Rutter, *Islets*, 2010, **2**, 49.
16 E. L. Que, R. Bleher, F. E. Duncan, B. Y. Kong, S. C. Gleber, S. Vogt, S. Chen, S. A. Garwin, A. R. Bayer and V. P. Dravid, *Nat. Chem.*, 2015, **7**, 130.
17 S. Iyoshi, M. Taki and Y. Yamamoto, *Org. Lett.*, 2011, **13**, 4558.
18 D. L. Li, S. W. Chen, E. A. Bellomo, A. I. Tarasov, C. Kaut, G. A. Rutter and W. H. Li, *Proc. Natl. Acad. Sci. U. S. A.*, 2011, **108**, 21063.
19 R. J. Radford, W. Chyan and S. J. Lippard, *Chem. Sci.*, 2013, **4**, 3080.
20 D. Li, Z. Huang, S. Chen, Z. Hu and W.-H. Li, *Bioconjugate Chem.*, 2015, **26**, 1443.
21 K. Rathore, C. S. Lim, Y. Lee, H. J. Park and B. R. Cho, *Asian J. Org. Chem.*, 2014, **3**, 1070.
22 D. Li, L. Liu and W.-H. Li, *ACS Chem. Biol.*, 2015, **10**, 1054.
23 Z. C. Xu, K. H. Baek, H. N. Kim, J. N. Cui, X. H. Qian, D. R. Spring, I. Shin and J. Yoon, *J. Am. Chem. Soc.*, 2010, **132**, 601.
24 F. Deng, S. S. Long, Q. L. Qiao and Z. C. Xu, *Chem. Commun.*, 2018, **54**, 6157.
25 W. She, K. Luo, C. Zhang, G. Wang, Y. Geng, L. Li, B. He and Z. Gu, *Biomaterials*, 2013, **34**, 1613.

